MATHEMATICAL ENGINEERING
TECHNICAL REPORTS

An Explicit Reconstruction Method for Magnetic Resonance Electrical Property Tomography Based on the Generalized Cauchy Formula

Takaaki NARA, Tesuya FURUICHI, and
Motofumi FUSHIMI

(Communicated by Takayasu MATSUO)

METR 2016–12 June 2016

DEPARTMENT OF MATHEMATICAL INFORMATICS
GRADUATE SCHOOL OF INFORMATION SCIENCE AND TECHNOLOGY
THE UNIVERSITY OF TOKYO
BUNKYO-KU, TOKYO 113-8656, JAPAN

WWW page: http://www.keisu.t.u-tokyo.ac.jp/research/techrep/index.html

An Explicit Reconstruction Method for Magnetic Resonance Electrical Property Tomography Based on the Generalized Cauchy Formula

Takaaki NARA, Tesuya FURUICHI, and Motofumi FUSHIMI

Department of Information Physics and Computing
Graduate School of Information Science and Technology
The University of Tokyo
{nara, furuichi, fushimi}@alab.t.u-tokyo.ac.jp

June, 2016

Abstract

This paper presents an explicit reconstruction formula for magnetic resonance electrical property tomography (MREPT). We derive a Dbar problem from the time-harmonic Maxwell equations under the assumptions that $H_z = 0$, $\partial H^+ \neq 0$, and $\partial_z H^+ = 0$, where the z-axis is parallel to the body axis, $H^+ \equiv \frac{1}{2}(H_x + iH_y)$ is the measured magnetic field, and $\partial \equiv \frac{1}{2}(\partial_x - i\partial_y)$. Then, by using the generalized Cauchy formula, the electrical conductivity and permittivity are explicitly expressed in terms of their boundary values and the measured magnetic field. We also propose an iterative algorithm based on the explicit reconstruction formula without the assumption that $\partial_z H^+ = 0$. Numerical simulations show that the proposed methods can reconstruct the conductivity even with noisy data.

1 Introduction

Recently, magnetic resonance electrical property tomography (MREPT) has attracted attention as an imaging modality that reconstructs the admittivity from radio-frequency (RF) magnetic fields measured by a magnetic resonance imaging (MRI) scanner. It can provide important diagnostic information, since the electrical conductivity and permittivity of cancerous tissues are different from those of normal tissues [9, 12, 15].

To formulate a problem, let $\gamma = \sigma + i\omega\epsilon$ be the admittivity to be reconstructed, where σ and ϵ are the electrical conductivity and permittivity, respectively, and ω is the Larmor frequency. We assume that the permeability inside the body is homogeneous and the same as that in the free

space, μ_0. Let $\boldsymbol{H}$ and $\boldsymbol{E}$ be the magnetic field and the electric field inside the body, respectively. Then, the governing equations are obtained from the time-harmonic Maxwell equations as

$$\begin{aligned} \nabla \times \boldsymbol{H} &= \gamma \boldsymbol{E}, & (1)\\ \nabla \times \boldsymbol{E} &= -i\omega\mu_0 \boldsymbol{H}, & (2)\\ \nabla \cdot \boldsymbol{H} &= 0. & (3) \end{aligned}$$

Taking the rotation of Eq. (1) and using Eqs. (1) through (3) gives

$$-\Delta \boldsymbol{H} = \frac{\nabla\gamma}{\gamma} \times (\nabla \times \boldsymbol{H}) - i\omega\mu_0\gamma \boldsymbol{H}, \quad (4)$$

which relates γ to $\boldsymbol{H}$. The observable quantity with an MRI scanner by using the so-called B1 mapping technique is not all the components of $\boldsymbol{H} = (H_x, H_y, H_z)^T$ but the positive rotating magnetic field $H^+ = \frac{1}{2}(H_x + iH_y)$, where the z-axis is parallel to the body axis (see, e.g., [5, 11, 15] and the references therein). The MREPT problem is to determine γ from the measured H^+.

For solving the MREPT inverse problem, a number of methods have been proposed. Assuming the local homogeneity of γ, Haacke *et al.* [3] neglected $\nabla\gamma$ in Eq. (4) to derive

$$\Delta \boldsymbol{H} = i\omega\mu_0\gamma \boldsymbol{H} \quad (5)$$

and obtained a direct reconstruction formula,

$$\gamma = \frac{\Delta H^+}{i\omega\mu_0 H^+}. \quad (6)$$

Katcher *et al.* [5] and Voigt *et al.* [13] proposed improving the stability by taking the local average of both sides of Eq. (5) by integration. However, the problem with these methods is that large errors occur where γ changes spatially [8].

Conventional approaches to removing the assumption of locally homogeneous admittivity may be categorized into two groups. The first approach is to obtain the spatial distribution of γ by solving a partial differential equation (PDE) numerically. Song *et al.* [10] derived a semilinear elliptic PDE which gives an implicit relation between inhomogeneous admittivity γ and H^+. Due to the nonlinearity of the PDE, they proposed an iterative algorithm under the assumptions that $H_z = 0$ and $\partial_z\gamma = 0$. Hafalir *et al.* [4] introduced the inverse of admittivity,

$$\lambda \equiv \frac{1}{\gamma},$$

and transformed Eq. (4) under the same assumptions ($H_z = 0$ and $\partial_z \gamma = 0$) into a linear PDE for λ:

$$(\partial_x H^+ - i\partial_y H^+)\partial_x \lambda + (i\partial_x H^+ + \partial_y H^+)\partial_y \lambda + \Delta H^+ \lambda - i\omega\mu_0 H^+ = 0. \quad (7)$$

They solved Eq. (7) with an appropriate boundary condition by a finite element method (FEM). Ammari *et al.* [1] derived a semi-elliptic PDE for γ without the assumption $\partial_z \gamma = 0$, and solved it with an optimization-based algorithm. A key issue for iterative methods is to provide a good initial estimate without which the local minimum solution can be obtained. For the first approach to solving PDEs, another problem is that the Laplacian of H^+ is included in the coefficients of the PDEs which may lead to large numerical errors when the data include noise.

The second approach is to derive an explicit, pointwise reconstruction formula. Nachman [6] took the inner product of Eq. (4) and $\nabla \times \boldsymbol{H}$, and thus obtained a direct reconstruction formula

$$\gamma = \frac{\Delta \boldsymbol{H} \cdot (\nabla \times \boldsymbol{H})}{i\omega\mu_0 \boldsymbol{H} \cdot (\nabla \times \boldsymbol{H})}.$$

However, besides the need to measure all the components of $\boldsymbol{H}$, which is not the case in practical MR scanners, this equation breaks down when $\boldsymbol{H} \cdot (\nabla \times \boldsymbol{H}) = 0$. Palamodov [7] assumed that $H_z = 0, \partial H^+ \neq 0$, and $\partial_z H^+ = 0$ and derived a PDE for λ:

$$\partial_{\bar{\zeta}} \lambda = -\lambda h_1 - h_2, \quad h_1 = -\frac{\Delta H^+}{2\partial_\zeta H^+}, \quad h_2 = \frac{i\omega\mu_0 H^+}{2\partial_\zeta H^+}, \quad (8)$$

where $\partial_\zeta = \frac{1}{2}(\partial_x - i\partial_y)$ and $\partial_{\bar{\zeta}} = \frac{1}{2}(\partial_x + i\partial_y)$, to which the general solution was given by

$$\lambda = -\exp(F)\left(\frac{1}{\pi\zeta} * \exp(-F)h_2 + f\right), \qquad F = \frac{1}{\pi\zeta} * h_1. \quad (9)$$

Here, $*$ represents the 2D convolution and f is a holomorphic function that satisfies the Riemann-Hilbert type problem (Eq. (12) in [7]) written with the boundary value of $\operatorname{Re}\lambda$. Then, by showing the relationship

$$\exp(-F)h_2 = \frac{i\omega\mu_0}{4}\partial_\zeta (H^+)^2, \quad (10)$$

and substituting Eq. (10) into Eq. (9), an expression of λ was derived (Eq. (11) in [7]):

$$\lambda = -\frac{i\omega\mu_0}{4}\frac{1}{\partial_\zeta (H^+)^2}\left(\frac{1}{\pi\zeta} * \partial_\zeta (H^+)^2 + f\right). \quad (11)$$

However, Eq. (10) is incorrect in that the dimensions of the left and right hand sides are different. In fact, they are $\mathsf{L}^2\mathsf{M}\mathsf{T}^{-3}\mathsf{I}^{-2}$ and $\mathsf{L}^{-2}\mathsf{M}\mathsf{T}^{-3}$, respectively, where $\mathsf{L}, \mathsf{M}, \mathsf{T}$ and I are the dimensions of length, mass, time, and electric current, respectively. Accordingly, Eq. (11) is incorrect.

In this paper, we derive an explicit reconstruction formula of the admittivity from the measured H^+ and a given boundary value of γ, assuming that $H_z = 0, \partial H^+ \neq 0$, and $\partial_z H^+ = 0$. First, we write Faraday's law in the form of a Dbar problem. Then, in a two-dimensional (2D) domain Ω representing a slice of a body, we apply the generalized Cauchy formula to express the z-component of the electric field E_z at an arbitrary position in Ω in terms of H^+ in Ω and the boundary value of γ on $\partial\Omega$. Finally, by using Ampere's law, γ is reconstructed from the ratio of $4\partial H^+$ to iE_z. An advantage of our method is that it gives an exact, explicit, pointwise reconstruction formula which does not require iterative computation nor the Laplacian of H^+. Furthermore, when we do not assume $\partial_z H^+ \neq 0$, an iterative algorithm that includes the effect of the changes in physical quantities with respect to the z-axis is derived in the basis of the explicit reconstruction formula. This method with low computational cost would provide an efficient way to obtain a good initial estimate for the conventional iterative methods.

This paper is organized as follows. In section 2.1, the governing equations are rewritten with the Dbar derivatives. After three assumptions and their physical meaning are presented in section 2.2, an explicit reconstruction formula of γ is derived in section 2.3. In section 2.4, we propose an iterative algorithm based on the explicit reconstruction method without the assumption $\partial_z H^+ \neq 0$. Section 3 is devoted to numerical simulations of the proposed algorithms. The paper is concluded in section 4.

2 Reconstruction formula based on the generalized Cauchy formula

2.1 Governing equations with the Dbar derivatives

First, we rewrite Maxwell's equations by using the notation

$$\partial \equiv \frac{1}{2}(\partial_x - i\partial_y), \quad \bar{\partial} \equiv \frac{1}{2}(\partial_x + i\partial_y), \quad H^+ \equiv \frac{1}{2}(H_x + iH_y), \quad E^+ \equiv \frac{1}{2}(E_x + iE_y).$$

Let us take the (x-component)+i (y-component) of Eq. (2). Then we have

$$(\partial_y E_z - \partial_z E_y) + i(\partial_z E_x - \partial_x E_z) = -i\omega\mu_0(H_x + iH_y),$$

which is rewritten as

$$\bar{\partial} E_z - \partial_z E^+ = \omega\mu_0 H^+. \tag{12}$$

Similarly, from the (x-component)+i (y-component) of Eq. (1), it holds that

$$\bar{\partial} H_z - \partial_z H^+ \;\; = \;\; i\gamma E^+. \tag{13}$$

Next, let us consider Eq. (3) + i (z-component of Eq. (2)). Then we have

$$(\partial_x H_x + \partial_y H_y + \partial_z H_z) + i(\partial_x H_y - \partial_y H_x) = i\gamma E_z,$$

which is rewritten as

$$4\partial H^+ + \partial_z H_z = i\gamma E_z. \tag{14}$$

Eqs. (12), (13), and (14) are the governing equations rewritten with the Dbar derivatives.

2.2 Assumptions

For Eqs. (12) through (14), we make the following assumptions.

- **Assumption 1**. $H_z = 0$
- **Assumption 2**. $\partial H^+ \neq 0$
- **Assumption 3**. $\partial_z H^+ = 0$

As pointed out in [4], the $|H_z|$ generated by a birdcage RF coil used in an MRI scanner is very small and can be neglected in its central regions. This is the basis of Assumption 1, and it is commonly assumed in the literatures [1, 7, 8, 10].

Assumption 2 is also typical for MREPT ([1, 7]). If $\partial H^+ = 0$, then from Eq. (14) with Assumption 1, we have $\gamma E_z = 0$, and hence $E_z = 0$ since $\gamma \neq 0$. In this case, γ cannot be determined from Eq. (14). Assumption 2 is necessary to avoid this situation. A Method for avoiding it and one for the case where $\partial H^+ \simeq 0$ are discussed in [4].

When Assumption 3 is assumed in addition to Assumption 1, from Eq. (13), it holds that

$$E^+ = 0, \tag{15}$$

that is, the electric currents flow only in the z-direction. This is the meaning of Assumption 3. It is assumed in Theorem 1 in [7]. We remark that in Theorem 2 in [7], a method is proposed that does not require Assumption 3.

In section 2.3, under Assumptions 1 through 3, we set Ω to be a 2D slice of a body and derive an explicit reconstruction formula of γ in terms of H^+ in Ω and γ on $\Gamma \equiv \partial\Omega$. An iterative algorithm that does not require Assumption 3 will be proposed in section 2.4.

2.3 Explicit reconstruction method

We now derive a reconstruction formula. From Eq. (14) with Assumption 1, we have

$$4\partial H^+ = i\gamma E_z. \tag{16}$$

As mentioned in section 2.2, from Assumptions 1 and 2 and $\gamma \neq 0$, it holds that $E_z \neq 0$, and hence

$$\gamma \;=\; \frac{4\partial H^+}{iE_z}. \tag{17}$$

To determine γ by using Eq. (17), we express E_z in terms of H^+ and the boundary value of E_z. For that purpose, let us substitute Eq. (15) into Eq. (12), then we have

$$\bar{\partial} E_z = \omega\mu_0 H^+. \tag{18}$$

This is the so-called Dbar problem. Generally, for a simply connected 2D domain Ω bounded by a simple closed contour $\Gamma = \partial\Omega$, if f is continuous on Γ and is a solution to a Dbar problem $\bar{\partial} f = g$, then the generalized Cauchy formula holds [2]:

$$f(w,\bar{w}) = \frac{1}{2\pi i}\int_\Gamma \frac{f(\zeta,\bar{\zeta})}{\zeta - w}d\zeta - \frac{1}{\pi}\int\int_\Omega \frac{g(\zeta,\bar{\zeta})}{\zeta - w}d\xi d\eta, \quad w \in \Omega, \tag{19}$$

where $\zeta = \xi + i\eta$. Note that the notation $f(w,\bar{w})$ is used for f at $w \in \Omega$, since it is not holomorphic when $g \neq 0$. Hence, for the Dbar problem (18), we obtain an expression for E_z at an arbitrary point $w \in \Omega$ in terms of its boundary value and H^+ in Ω as follows:

$$E_z(w,\bar{w}) \;=\; \frac{1}{2\pi i}\int_\Gamma \frac{E_z(\zeta,\bar{\zeta})}{\zeta - w}d\zeta - \frac{\omega\mu_0}{\pi}\int\int_\Omega \frac{H^+(\zeta,\bar{\zeta})}{\zeta - w}d\xi d\eta, \quad w \in \Omega. \tag{20}$$

Here, from Eq. (16), E_z on Γ can be replaced with $\frac{4\partial H^+}{i\gamma}$, so that we have

$$E_z(w,\bar{w}) \;=\; -\frac{1}{\pi}\int_\Gamma \frac{\frac{2}{\gamma}\partial H^+}{\zeta - w}d\zeta - \frac{\omega\mu_0}{\pi}\int\int_\Omega \frac{H^+(\zeta,\bar{\zeta})}{\zeta - w}d\xi d\eta, \quad w \in \Omega. \tag{21}$$

By substituting Eq. (21) into Eq. (17), we arrive at

$$\gamma(w,\bar{w}) \;=\; \frac{4\pi i\partial H^+(w,\bar{w})}{\displaystyle\int_\Gamma \frac{\frac{2}{\gamma(\zeta,\bar{\zeta})}\partial H^+(\zeta,\bar{\zeta})}{\zeta - w}d\zeta + \omega\mu_0\int\int_\Omega \frac{H^+(\zeta,\bar{\zeta})}{\zeta - w}d\xi d\eta}, \quad w \in \Omega. \tag{22}$$

Eq. (22) is our explicit reconstruction formula for an inhomogeneous γ, under the assumptions $H_z = 0$, $\partial H^+ \neq 0$, and $\partial_z H^+ = 0$; it does not include the Laplacian of H^+ or any arbitrary parameters and it enables us to compute γ point by point from the measured H^+ and the boundary value of γ.

As in [1, 4, 7], we assume that γ on Γ is given. We note that in practical situations, the Dirichlet boundary condition could be given in the following two ways. First, as in [1], we assume γ is a constant and that it is known *a priori* near the body surface where Γ is set. Second, Ω is taken as a local region of interest (ROI) inside which it is possible that a small cancer exists, and γ on its boundary is set to be that of normal tissue.

2.4 A reconstruction algorithm without Assumption 3: $\partial_z H^+ = 0$

Next, we consider an algorithm that does not require Assumption 3. We assume that H^+ is measured on several planes $z = z_n\,(n = 1, \cdots, N)$. In this case, from Eq. (13) with Assumption 1, it holds that

$$E^+ = \frac{i\partial_z H^+}{\gamma} \quad (\neq 0), \tag{23}$$

and we should take $\partial_z E^+$ into account in Eq. (12). Eq. (23) shows that, once γ is obtained, E^+ can be computed on several planes that have different z-coordinates, from which $\partial_z E^+$ can be also computed. We now propose the following algorithm.

1) Ignore $\partial_z E^+$ first, and obtain an initial estimate of γ by using the explicit reconstruction formula (22) for each plane $z = z_n\,(n = 1, \cdots, N)$.

2) With the reconstructed γ, compute E^+ by using Eq. (23).

3) Compute $\partial_z E^+$ and substitute it into

$$\bar{\partial} E_z = \omega\mu_0 H^+ + \partial_z E^+, \tag{24}$$

which gives a renewed Dbar problem that includes the effect of $\partial_z E^+$. The corrected value of γ is then obtained by

$$\gamma(w, \bar{w}) = \frac{4\pi i \partial H^+(w, \bar{w})}{\displaystyle\int_\Gamma \frac{\frac{2}{\gamma}\partial H^+}{\zeta - w} d\zeta + \int\int_\Omega \frac{\omega\mu_0 H^+(\zeta, \bar{\zeta}) + \partial_z E^+(\zeta, \bar{\zeta})}{\zeta - w} d\xi d\eta}. \tag{25}$$

Go back to 2), if necessary.

3 Numerical verification

3.1 Explicit reconstruction formula (22)

In this section, we numerically verify the reconstruction formula (22). We compare our method with one that uses Eq. (6) which, following [4], we call "std-MREPT method".

As shown in Fig. 1 (Model 1), we examined a model composed of three cylinders (conductivity : 1 S/m, radii: 5 mm, 10 mm, 15 mm) embedded in a cylinder (conductivity: 0.5 S/m, radius: 100 mm). The height and the relative permittivity of each of the cylinders were 2000 mm ($-1000 \leq z \leq 1000$ mm) and 80, respectively. A plane wave with a frequency of 64 MHz where $\boldsymbol{H}$ and $\boldsymbol{E}$ were parallel to the y and z-axes, respectively, was input from the negative to the positive x-axis direction. A forward solution was computed by an FEM software, ANSYS HFSS (ANSYS Japan). Ω was defined to be 136 mm by 136 mm square centered at the origin in the plane $z = 0$. In Ω, 68 by 68 pixels were set; the resolution was 2 mm. Gaussian noises was added to both the real and the imaginary parts of H^+. We let d be the ratio of the standard deviation of the noise to that of $|H^+|$ in Ω, and we examined the cases where $d = 0$ (noiseless) and $d = 0.01$. To compute ∂H^+ at the pixel (l, m), as in [4], we used a second-order polynomial as a local approximation to H^+. Specifically, for the 3×3 pixels centered at (l, m), H^+ was approximated by the second-degree polynomial $H^+_{lm} \simeq c_{00}+c_{10}x_{lm}+c_{01}y_{lm}+c_{20}x^2_{lm}+2c_{11}x_{lm}y_{lm}+c_{02}y^2_{lm}$, from which we obtained an approximation for ∂H^+ as $\partial H^+_{l,m} \simeq \frac{1}{2}((c_{10} + 2c_{20}x_{lm} + 2c_{11}y_{lm}) - i(c_{01} + 2c_{11}x_{lm} + 2c_{02}y_{lm}))$.

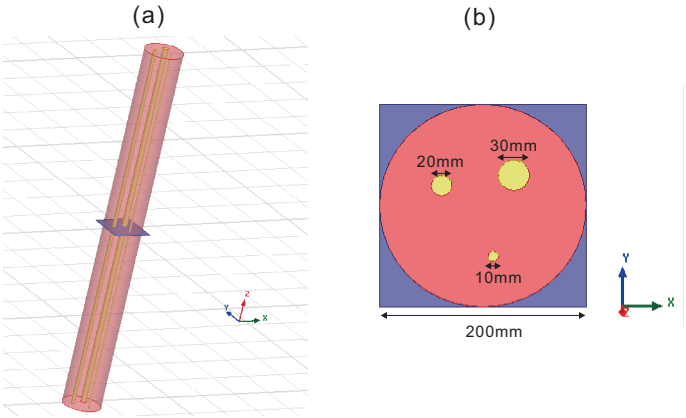

Figure 1: Model 1: three cylinders (conductivity: 1S/m) were embedded in a cylinder (conductivity: 0.5S/m)

Note that in the integral of H^+ over Ω in Eq. (22), it holds that

$$\int\int_{U_\epsilon(w)} \frac{H^+(\zeta,\bar{\zeta})}{\zeta - w} d\xi d\eta = 0, \tag{26}$$

where $U_\epsilon(w)$ is a circle centered at w with a radius of ϵ. Because of this, we remove H^+ at pixel including w and use the values at the other $68^2 - 1$ pixels when numerically computing $\int\int_\Omega \frac{H^+}{\zeta - w} d\xi d\eta$.

Fig. 2 (a) and (b) show the reconstructed conductivity when $d = 0$ by our method and the std-MREPT method, respectively. Our method performed a good reconstruction of the domains with higher conductivity, irrespective of the diameter of the domain, while in the std-MREPT method large errors were observed on the boundary, where the conductivity is discontinuous. Fig. 2 (c) and (d) show the reconstructed conductivity when $d = 0.01$ by our method and the std-MREPT method, respectively. The std-MREPT method, which requires the computation of the Laplacian of H^+, was unable to reconstruct the distribution of γ due to noise; in contrast, in each of the three domains, the conductivity estimated by our method was higher than that of the background even with noisy data. Note that the range of the electrical conductivity in Fig. (b) and (d) was restricted from -5 to 5 S/m for visibility, although the maximum of the absolute values in Fig. (b) and (d) were about 50 and 400, respectively.

3.2 Algorithm in section 2.4

To evaluate the effectiveness of the algorithm presented in section 2.4 when $\partial_z \gamma \neq 0$ and hence $\partial_z H^+ \neq 0$, we performed a simulation of the following, which we call Model 2: a short cylinder (conductivity: 0.5S/m; radius: 10 mm) with the length of 20 mm was inserted coaxially in another cylinder (conductivity: 0.25S/m; radius: 200 mm; length: 2000 mm) such that $-10 < z < 10$ mm. In this case, γ changes discontinuously along the z-axis at $z = \pm 10$ mm. We assumed that H^+ was observed at ten different layers, where $z = 0, 2, \cdots, 18, 20$ mm. To compute $\partial_z E^+$ at (l, m, n) in step 3) in the algorithm, we took $3 \times 3 \times 3$ pixels around (l, m, n) and approximated E^+ by the second-degree polynomial $E^+_{l,m,n} = d_{000} + d_{100}x_{lmn} + d_{010}y_{lmn} + d_{001}z_{lmn} + d_{200}x^2_{lmn} + d_{020}y^2_{lmn} + d_{002}z^2_{lmn} + 2d_{110}x_{lmn}y_{lmn} + 2d_{011}y_{lmn}z_{lmn} + 2d_{101}z_{lmn}x_{lmn}$ from which we obtained $\partial_z E^+_{l,m,n} \simeq d_{001} + 2d_{002}z_{lmn} + 2d_{011}y_{lmn} + 2d_{101}x_{lmn}$.

First, we examined the noiseless case ($d = 0$). Fig. 3 shows the true conductivity at $z = 8$ mm and 12 mm, the conductivity estimated by the explicit reconstruction method using Eq. (22), and the conductivity reconstructed using a single application of the steps 2) and 3) of the algorithm presented in section 2.4 for an initial estimate given by Eq. (22). We observe that although the conductivity obtained by the explicit reconstruction method

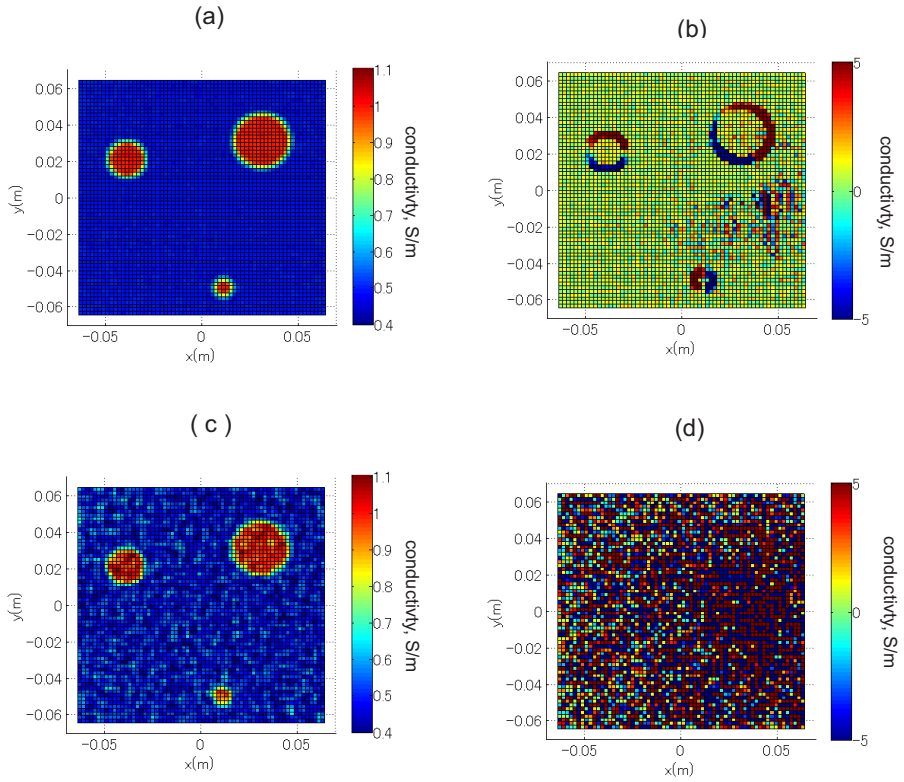

Figure 2: Numerical simulation: (a) estimated by the proposed method without noise ($d = 0$), (b) estimated by the std-MREPT method without noise ($d = 0$), (c) estimated by the proposed method ($d = 0.01$), (d) estimated by the std-MREPT ($d = 0.01$).

reflected the true values, these results were improved by the correction steps 2) and 3) of the algorithm in section 2.4.

Fig. 4 shows the results when $d = 0.01$. Even in this case, at $z = 8$ mm, including the corrections clarifies the domain where the conductivity is different from the background.

The left and right panels of Fig. 5 show the conductivity along the z-axis when $d = 0$ and $d = 0.01$, respectively. We observe in both cases that the reconstructed values are improved by the algorithm in section 2.4, which takes $\partial_z E^+$ into account. This approach has a low computational cost and could be used as an initial solution for an optimization algorithm such as that presented in [1].

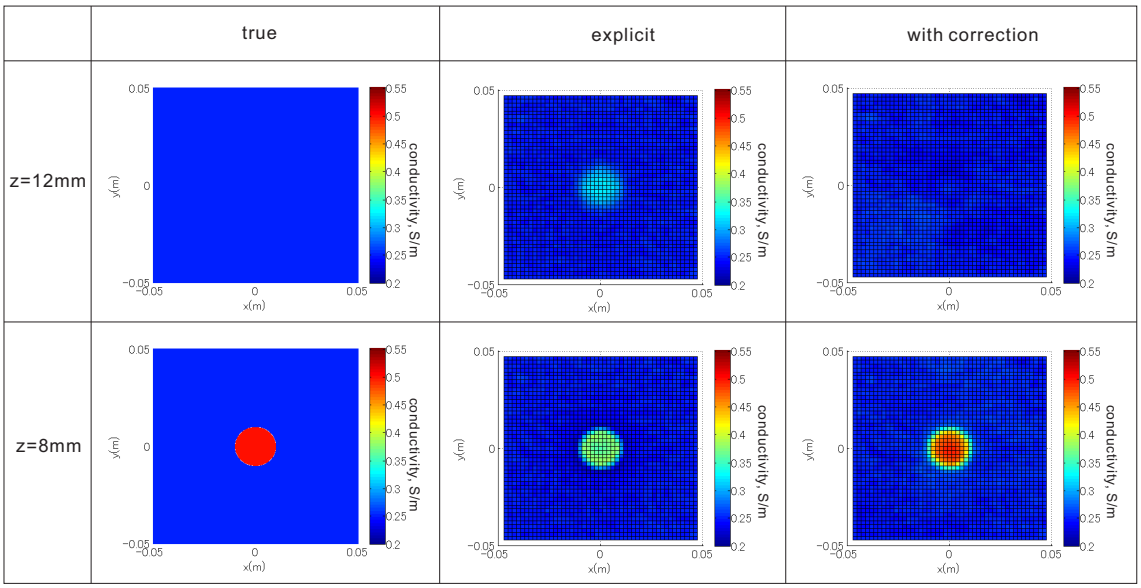

Figure 3: Reconstructed conductivity of a short cylinder at $z = 8, 12$ mm when $d = 0$: (left column) true conductivity, (center column) the conductivity estimated by the explicit reconstruction method using Eq. (22), (right column) the conductivity after applying steps 2) and 3) of the algorithm presented in section 2.4.

4 Conclusion

In this paper, we derived an explicit reconstruction formula for MREPT. Assuming that $H_z = 0$, $\partial H^+ \neq 0$, and $\partial_z H^+ = 0$, an explicit, pointwise reconstruction formula for the admittivity was derived by using the generalized Cauchy formula for a Dbar problem. As an extension of this, we also

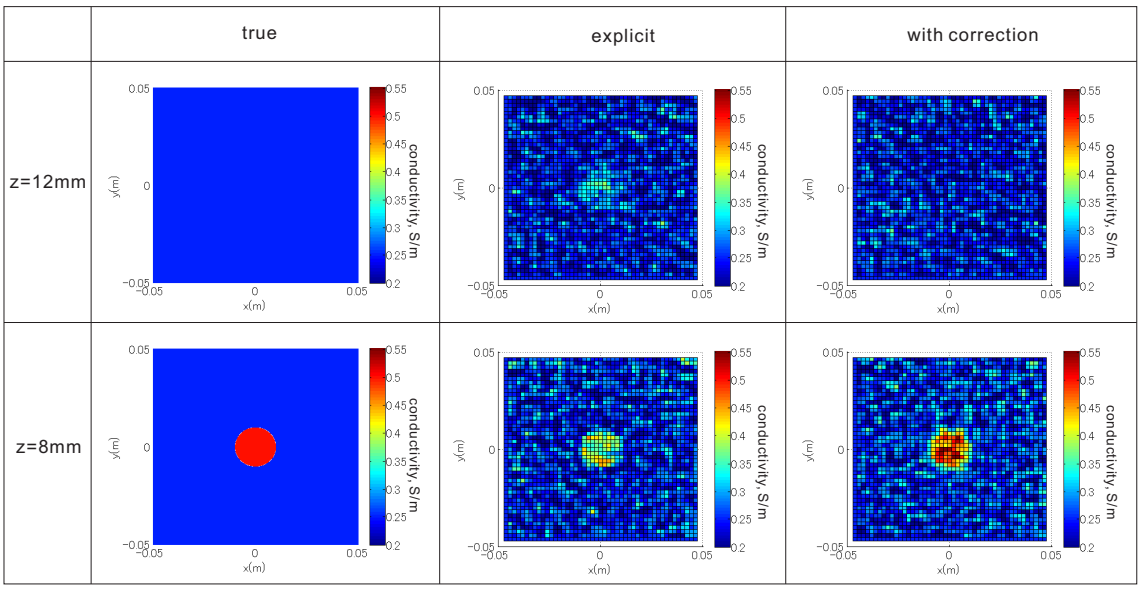

Figure 4: Results when $d = 0.01$.

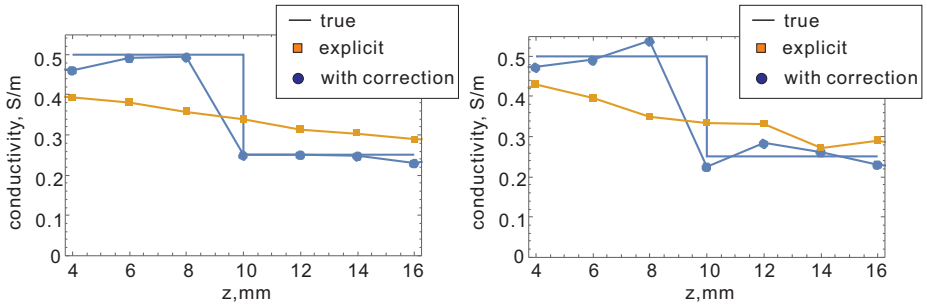

Figure 5: Reconstructed conductivity along the z-axis before and after applying the correction given in the algorithm presented in section 2.4: (left) $d = 0$ (noiseless), (right) $d = 0.01$.

proposed an algorithm that does not require the assumption that $\partial_z H^+ = 0$. Both algorithms were verified numerically.

Acknowledgement

This work was supported by JSPS Grant-in-Aid for Scientific Research on Innovative Areas (Multidisciplinary Computational Anatomy) JSPS KAKENHI Grant Number 26108003.

References

References

[1] Ammari, H., Kwon, H, Lee, Y., Kang, K., and Seo, J. K., Magnetic resonance-based reconstruction method of conductivity and permittivity distributions at the Larmor frequency, Inverse Problems, 31, 105001, 2015.

[2] Ablowitz, M. J. and Fokas, A. S., Complex variables, Introduction and Applications, Second edition, Cambridge University Press, 2003.

[3] Haacke, E. M., Petropoulos, L. S., Nilges, E. W., and Wu, D. H., Extraction of conductivity and permittivity using magnetic resonance imaging, Physics in Medicine and Biology, 38, 6, 471-477, 1991.

[4] Hafalir, F. S., Oran, O. F., Gurler, N, and Ider, Y. Z., Convection-Reaction Equation based Magnetic Resonance Electrical Properties Tomography (cr-MREPT), IEEE Trans. Medical Imaging, 33, 777-793, 2014.

[5] Katscher, U., Voigt, T., Findeklee, C., Vernickel, P., Nehrke, K., and Dossel, O., Determination of electrical conductivity and local SAR via B1 mapping, IEEE Trans. Medical Imaging, 28, 9, 1365-1374, 2009.

[6] Nachman, A., Wang, D., Ma, W., and Joy, M., A local formula for inhomogeneous complex conductivity as a function of the RF magnetic field, ISMRM 15th Sci. Meeting Exhibit., Germany, 2007.

[7] Palamodov, V., An analytic method for the inverse problem of MREPT, Inverse Problems, 32, 035003, 2016.

[8] Seo, J. K., Kim, M.-O., Lee, J., Choi, N., Woo, E. J., Kim, H. J., Kwon, O. I., and Kim, D.-H., Error analysis of nonconstant admittivity for MR-based electric property imaging, IEEE Trans. Medical Imaging, 31, 2, 430-437, 2012.

[9] Shin, J., Kim, M. J., Lee, J., Nam, Y., Kim, M-O., Choi, N., Kim, S., and Kim, D-H., Initial study on in vivo conductivity mapping of breast cancer using MRI, Journal of Magnetic Resonance Imaging, 42, 371-378, 2015.

[10] Song, Y. and Seo, J. K., Conductivity and permittivity image reconstruction at the Larmor frequency using MRI, SIAM Journal on Applied Mathematics, 73, 6, 2262-2280, 2013.

[11] Stollberger, R. and Wach, P., Imaging of the active B_1 field in vivo, Magnetic Resonance in Medicine, 35, 246-251, 1996.

[12] Surowiec, A. J., Stuchly, S. S., Barr, J. R., and Swarup, A., Dielectric properties of breast carcinoma and the surrounding tissues, IEEE Trans. Biomed. Eng., 35, 257-263, 1988.

[13] Voigt, T., Katscher, U., and Doessel, O., Quantitative conductivity and permittivity imaging of the human brain using electric properties tomography, Magnetic Resonance in Medicine, 66, 456-466, 2011.

[14] Zhang, X., Zhu, S., and He, B., Imaging electric properties of biological tissues by RF field mapping in MRI, IEEE Trans. Medical Imaging, 29, 474-481, 2010.

[15] Zhang, X., Liu, J., and He, B., Magnetic-resonance-based electrical properties tomography: a review, IEEE Reviews in Biomedical Engineering, 7, 87-96, 2014.